Development of a yield sensor for measuring individual weights of onion bulbs

Qarallah, Bassam

Shoji, Koichi

Kawamura, Tsuneo

(Citation)
Biosystems Engineering,100(4):511-515

(Issue Date)
2008-10

(Resource Type)
journal article

(Version)
Accepted Manuscript

(URL)
https://hdl.handle.net/20.500.14094/90000979

Development of Yield Sensor for Measuring Individual Weights of Onion Bulbs

Bassam Qarallah[a], Koichi Shoji[a,*], Tsuneo Kawamura[a]

[a]Graduate School of Agriculture, Kobe University, 1-1 Rokkodai-cho, Nada-ku, Kobe, 657-8501, Japan

[*]Corresponding author. E-mail address: shojik@kobe-u.ac.jp

Abstract

Site-specific measurement of the weight of individual tubers, bulbs and fruits on the harvester may enhance their market value and represent a significant advance for precision agriculture. An impact-based yield sensor was developed, consisting of two load cells, an acrylic plate and a polyurethane cushion, to determine the weight of individual onion bulbs through the impulse received by the sensor. A simple proportional relation was used to calibrate the sensitivity of the sensor, the precision of which was evaluated by standard and relative errors at calibration and validation. The experimental variables investigated under static conditions were the arrangement of the bulbs on the conveyor, the thickness of the cushion on the plate, and the clearance between the output end of the conveyor and the impact plate. The arrangement of the bulbs affected neither the precision nor the sensitivity of the sensor. With or without a 10 mm-thick cushion on the plate, the precision decreased at the higher clearance. Practical precision was obtained (a relative error at validation of less than 2.0%) with a 30 mm- thick cushion regardless of the clearance.

1. Introduction

Yield monitoring, an important technique in precision farming, is exercised for measuring, spatially referencing and mapping yield variation within fields. Following the commercial availability of yield monitors for grain crops, yield monitors based on

mass flow have been developed for the measurement of non-grain crops such as potatoes (Ehlert, 2000; Hara *et al.*, 2003) and citrus fruits (Grift *et al.*, 2006). Either an optical sensor or a load cell has been used for such measurements.

When handling such high-value crops, however, monitoring the weight of each tuber, bulb or fruit will be important for the next generation of precision agriculture. When the distribution of the size, or in practice the weight, of each product is known throughout the field, site-specific management will widen the options to optimize cultural practices. Variable planting density will be applicable to most tuberous and bulbar annual crops, variable pruning and thinning intensity to fruit trees, and variable selection of the age of seed tubers to potatoes. These measures for controlling individual size are primarily aimed at enhancing market value; however, the necessary information cannot be obtained through existing yield sensors that monitor only total weight or flow rate (*e.g.* Ehlert, 2000; Hara *et al.*, 2003) of the product on the harvester.

There are some individual measurement techniques for quality evaluation of products. For example, Schueller and Wall (1991) have developed theory and procedures to detect elasticity (firmness, thereby ripeness) of fruit dropping on a simply supported beam. De Baerdemaeker *et al.* (1982) have measured firmness by frequency spectrum analysis of the signal of the impact occurring when dropping the product on a plate. However, examples of individual measurement of weight or size are limited. Hofstee and Molema (2002; 2003) have estimated the volume of individual potato tubers using machine vision on the conveyor of a harvester. Tokunaga and Shoji (2006) have determined the individual weight of potato tubers by an impact-based sensor.

The objective of this study is to develop a simple yield sensor capable of determining the weights of individual units of large-size crops on the harvester. The onion, a typical

bulbar crop, was selected for the present investigation. Its irregular shape including the roots and the apex is a challenge in the development of such a sensor. When successfully applicable to the onion, the sensor would readily be applicable to other products of more regular shape, such as potatoes and oranges.

2. Materials and methods

2.1. *Onion bulbs and their arrangement on the conveyor*

A group of 25 stored onion bulbs of “Momiji-Sangou” cultivars, weighing between 183 g and 369 g each, was used in each measurement. The bulbs were placed on a conveyor belt [250 mm (W) × 2500 mm (L)] moving at a speed of 0.15 m s^{-1}, as specified in a commercial-use onion picker used in Hyogo Prefecture and its environs (Kansai Region), Japan. The bulbs were placed near the centre of the conveyor, with their arrangements considered as an experimental factor: “Forward” (the base), “Backward” (the apex) and “Perpendicular” (the scale) facing the output end of the conveyer [Fig. 1, (a)].

2.2. *Impact plate and cushion.*

The impact plate [Fig. 1, (c)] was placed at an angle of 37° to the horizontal plane beneath the output end of the conveyor. This angle was empirically determined to avoid double impacts of the same bulb and accumulation of debris on the plate.

The plate comprised a polyurethane cushion affixed to an acrylic plate (300 mm × 180 mm × 5 mm). The thickness of the cushion was varied to 0 mm, 10 mm, and 30 mm.

2.3. *Clearance*

Clearance, the vertical (*H*) and horizontal (*S*) distances (mm) between the output end of the conveyor and the centre of the impact cushion [Fig. 1, (d)], was set at two levels

of “Low” (110, 125) and “High” (136, 180).

2.4. *Load cell and data acquisition*

Two rectangular-ring load cells as described by Shoji *et al.* (2002) supported the impact plate [Fig. 1, (c)] and were located 200 mm apart. The sensitivities of each load cell were 18.95 N mV^{-1} and 18.45 N mV^{-1} under the input voltage of the bridge circuit of 2.0 V. Upon the impact of a bulb, natural frequency was observed around 260 Hz associated with the spring-mass system of the load cell and the plate, and another around 100 Hz attributable to the vibration of the plate itself supported by the load cells. The signals were recorded at 1 kHz, and an eighth-order Butterworth low-pass filter (-160 dB dec^{-1}) was subsequently applied at 50 Hz. The output of each impact was integrated to calculate impulse p to relate to the weight of the bulb as below:

$$p = \int_0^{t_1} F(t)dt = \frac{1}{f_s}\sum_{i=1}^{t_1 f_s} F_i \qquad \ldots(1),$$

where F is the force on the sensor, f_s the sampling frequency, t the time elapsed from the start of an impact, and i the sample number counted from the start. The duration of the integration t_1 was set at 100 ms, within which damped vibration, if applicable, of the signal mostly disappeared. Both positive and negative signals were integrated, as this procedure had resulted in better calibration than integrating either side of the signal.

2.5. *Experimental design and analysis*

The arrangement of the bulbs, the thickness of the cushion and the clearance were taken as the experimental factors, for a total of 18 ($3\times3\times2$) measurements, without replication.

At each measurement, 9 of 25 pairs (pair: weight and impulse) of data were used for calibration by the following proportional relation:

$$w = ap \qquad \ldots(2),$$

where w is the weight of bulb, p the impulse received by the sensor, and a the calibrated parameter by the least-squares method. The remaining 16 pairs were used for validation.

Coefficient of determination (R^2) for calibration, root-mean squared error (hereinafter "standard error") and root-mean squared relative error (hereinafter "relative error") at both calibration and validation, and relative error of the total estimated weight at validation (hereinafter "total error") were calculated accordingly. The sensitivity of the sensor, which was nearly equal to the inverse of parameter a, was also calibrated from the inverse relation of Eqn (2).

Analysis of variance (ANOVA) without interaction of the factors was conducted using the above indicators as characteristic values, except R^2 and the total error. Before the analysis, the values were converted to approach to normal distribution. The following functions were selected for sensitivity:

$$y = (x - \bar{x})^3 \qquad \ldots(3),$$

and for standard and relative errors of calibration and validation:

$$y = \log_e x \qquad \ldots(4),$$

where x is the characteristic value, $\bar{x}$ the grand average, y the converted value for ANOVA. Multiple comparisons were conducted for the averages of the applicable factors with three levels.

3. Results and discussion

3.1. *Adequacy of calibration model*

The proportional relation assumed in Eqn (2) was appropriate. Other calibration models, such as the linear relation with intercept or the power of the impulse, were also tested, but neither the intercept nor the non-linearity of the models was statistically

confirmed. The total error was within ±5% throughout the measurements (Table 1, last column), implying that the residuals associated with the proportional model were not markedly biased. The standard and relative errors between the calibration and the validation were similar (Table 1, sixth to ninth columns), indicating that the model was stable at each measurement.

Although the calibration and the validation plots dispersed in some cases (Fig. 2, unfilled symbols), they showed practical applicability of the sensor with the 30 mm cushion (Fig. 2, filled symbols).

3.2. *Arrangement of the bulbs*

The arrangement of the bulbs on the conveyor was not a significant factor in terms of the precision of the sensor, as demonstrated by the standard and relative errors (Table 2, fifth to eighth columns). Although controlled as an experimental factor, the impact of the bulbs occurred mainly on the scale side or the base [Fig. 1, (b)].

The sensitivity of the sensor was not affected by the arrangement either (Table 2, third column). This, however, is advantageous in practical applications for insuring the stability of the output, since the arrangement of the bulbs is not easily controlled on the harvester.

3.3. *Thickness of cushion*

The thickness of the polyurethane cushion was clearly a significant factor affecting the precision of the sensor (Table 2, fifth to eighth columns). The precision tended to be higher with a thicker cushion (Table 1, sixth to ninth columns), although the difference in precision between 0 mm and 10 mm cushions was not statistically significant (Table 2).

In contrast, the sensitivity of the sensor increased significantly by simply attaching

even the 10 mm cushion (Table 2, third column). Part of the reason for this increase was that the depression of the cushion formed by the impact of the bulb added to the clearance [the distances to the surface of the cushion: Fig. 1, (d)] resulted in a practically longer vertical distance from the output end of the conveyor to the sensor and imparted a higher velocity to the bulb.

3.4. *Clearance*

The high clearance lessened the precision of the sensor, although less significantly than did the thickness of the cushion (Table 2, fifth to eighth columns). This was attributed to the interaction between clearance and thickness; the standard and relative errors were low with the 30 mm cushion regardless of clearances (Table 1, sixth to ninth columns).

The sensitivity of the sensor was significantly higher at the high clearance (Table 2, third column) due to the greater velocity upon impact. The values were distributed near either of the averages (2.95 or 3.29) throughout the measurements (Table 1, fourth column), to which Eqn (3) was specifically applied to approach to normal distribution before ANOVA. In view of the effect of the thickness on the sensitivity (section 3.3), the clearance mainly affected the sensitivity of the sensor.

3.5. *Waveforms of impact affected by thickness of cushion*

With the 0 mm and 10 mm cushions, a backlash was observed in the waveforms after the first peak (Fig. 3), resulting in short-term damped vibration, although the vibration of the higher frequency (ca. 100 Hz) and of the greater amplitude had been cut off by the low-pass filter set at 50 Hz. This indicated that the acrylic plate was deformed and then reformed after the impact. Particularly, with the 10 mm cushion, most of the bulbs depressed the cushion completely to deform the plate and to produce a waveform

similar to that with the 0 mm cushion.

The 30 mm cushion generated a lower peak and a gradual drop in the force of the impact (Fig. 3). Notably, the damped vibration did not appear, indicating that the acrylic plate was not affected because the cushion was not fully depressed upon impact.

3.6. *Direction of the bound and precision of the sensor*

Video images taken at each measurement demonstrated that, with the 0 mm or 10 mm cushions, some bulbs bounced further downward and some upward. Those bouncing downward obviously imparted a lower impulse to the sensor, which consequently lessened the precision of the sensor. Such variability in the direction of the bound arose from the random rotation of the bulbs upon impact, and the torque requisite for the rotation was assumed to be generated from the reaction force from the sensor whose line of action deviated from the centre of gravity of the bulbs because of their irregular shape. Irregular bounds were more frequently observed at the high clearance, although the reason for this is still unclear.

In contrast, with the 30 mm cushion, the direction of the bound after impact was almost consistent, regardless of which side of the bulb impacted the sensor. The cushion was not fully depressed (section 3.5) and generated a reaction force distributed on the surface of bulbs, which was assumed to limit their rotation and to produce a consistent direction upon bouncing. The direction remained consistent even at the high clearance, and the precision of the sensor was accordingly maintained (section 3.3; Table 1, sixth to ninth columns).

4. Conclusions

1. An impact-based yield sensor consisting of two load cells, an acrylic plate and a polyurethane cushion was designed for measuring the individual weights of onion

bulbs.

2. The arrangement of the bulbs on the conveyor affected neither the precision nor the sensitivity of the sensor.
3. An increase in the clearance between the output end of the conveyor and the sensor resulted in less precision, with a 0 mm or a 10 mm cushion.
4. The precision of the sensor was maintained with a 30 mm cushion even at the high clearance, resulting in a relative error of less than 2.0% at validation.
5. The sensitivity of the sensor was affected mainly by and increased with the clearance.

References

De Baerdemaeker J; Lemaitre L; Meire, R (1982). Quality detection by frequency spectrum analysis of the fruit impact force. Transactions of the ASAE, 25(1), 175-178

Ehlert D (2000). Measuring mass flow by bounce plate for yield mapping of potatoes. Precision Agriculture, 2(2), 119-130

Grift T; Ehsani R; Nishiwaki K; Crespi C; Min M (2006). Development of a yield monitor for citrus fruits, ASABE Paper, 061192

Hara Y; Takenaka H; Sekiguchi K (2003). Poteto-habesta you shuryou sensa oyobi shuryou sokutei shisutemu no kaihatsu (Study on potato yield sensor and monitoring system for potato harvester). Journal of the Japanese Society of Agricultural Machinery, 65(6), 158-162

Hofstee J W; Molema G J (2002). Machine vision based yield mapping of potatoes. ASAE Paper 02-1200

Hofstee J W; Molema G J (2003). Volume estimation of potatoes partly covered with

dirt tare. ASAE Paper 031001

Schueller, J K; Wall T M P (1991). Transverse impact of fruit on beams to determine modulus of elasticity. Experimental Mechanics, 31(2), 118-121

Shoji K; Kawamura T; Horio H (2002). Impact-based grain yield sensor with compensation for vibration and drift. Journal of Japanese Society of Agricultural Machinery, 64(5), 108-115

Tokunaga J; Shoji K (2006). Development of potato yield sensor to measure the mass of individual tubers. Preprints of 3rd IFAC International Workshop on Bio-Robotics, Information Technology and Intelligent Control for Bioproduction Systems (Bio-Robotics III), pp 239-243, Sapporo, Japan

Table 1 - Experimental factors, levels and statistical indicators for calibrations and validations

Experimental factor			Calibration (n=9)				Validation (n=16)		
Thickness of cushion, mm	Arrangement of bulbs	Clearance	Sensitivity, mN g^{-1}	R^2	Standard error, g	Relative error, %	Standard error, g	Relative error, %	Total error, %
0	Forward	Low	2.92	0.967	11.4	4.6	13.2	4.3	-2.4
		High	3.22	0.757	30.9	11.0	22.2	7.4	-2.0
	Backward	Low	2.89	0.990	6.2	2.3	14.8	5.1	+1.8
		High	3.24	0.806	27.6	9.2	20.8	7.0	-1.2
	Perpendicular	Low	2.93	0.968	11.2	4.7	14.3	5.0	-2.3
		High	3.17	0.857	23.7	12.0	21.3	6.7	+4.9
10	Forward	Low	3.01	0.951	13.9	4.9	11.8	4.1	-3.3
		High	3.34	0.891	20.8	8.9	26.1	8.9	-2.3
	Backward	Low	2.93	0.977	9.5	3.8	8.4	2.8	-1.0
		High	3.28	0.847	24.5	7.3	19.4	6.5	-4.1
	Perpendicular	Low	2.93	0.984	8.0	2.9	8.5	2.7	+1.3
		High	3.33	0.849	24.4	8.5	20.1	6.7	-2.3
30	Forward	Low	2.96	0.991	5.9	2.4	5.0	1.7	+0.6
		High	3.33	0.995	4.3	1.6	5.3	1.8	+0.2
	Backward	Low	3.00	0.993	5.3	1.8	5.0	1.6	-0.1
		High	3.35	0.992	5.7	1.8	6.0	2.0	+0.5
	Perpendicular	Low	2.96	0.988	6.9	2.4	4.3	1.4	+0.4
		High	3.33	0.996	3.8	1.2	4.2	1.4	+0.2

Table 2 - Averages of the statistical indicators for each level of the experimental factors

Experimental factor	Level	Calibration (n=9)				Validation (n=16)	
		Sensitivity, mN g^{-1}	R^2	Standard error, g	Relative error, %	Standard error, g	Relative error, %
Arrangement of bulbs	Forward	3.13	0.925	14.5	5.6	14.0	4.7
	Backward	3.11	0.934	13.1	4.4	12.4	4.2
	Perpendicular	3.11	0.940	13.0	5.3	12.1	4.0
Thickness of cushion	0 mm	3.06 [a]	0.891	18.5 [a]	7.3 [a]	17.8 [a]	5.9 [a]
	10 mm	3.14 [b]	0.917	16.8 [a]	6.1 [a]	15.7 [a]	5.3 [a]
	30 mm	3.15 [b]	0.993	5.3 [b]	1.9 [b]	5.0 [b]	1.6 [b]
Clearance	Low	2.95 [a]	0.979	8.7 [a]	3.3 [a]	9.5 [a]	3.2 [a]
	High	3.29 [b]	0.888	18.4 [b]	6.8 [b]	16.2 [b]	5.4 [b]

[a b] Different superscripts indicate differences in the averages compared within the factor at a significance level of 5%.

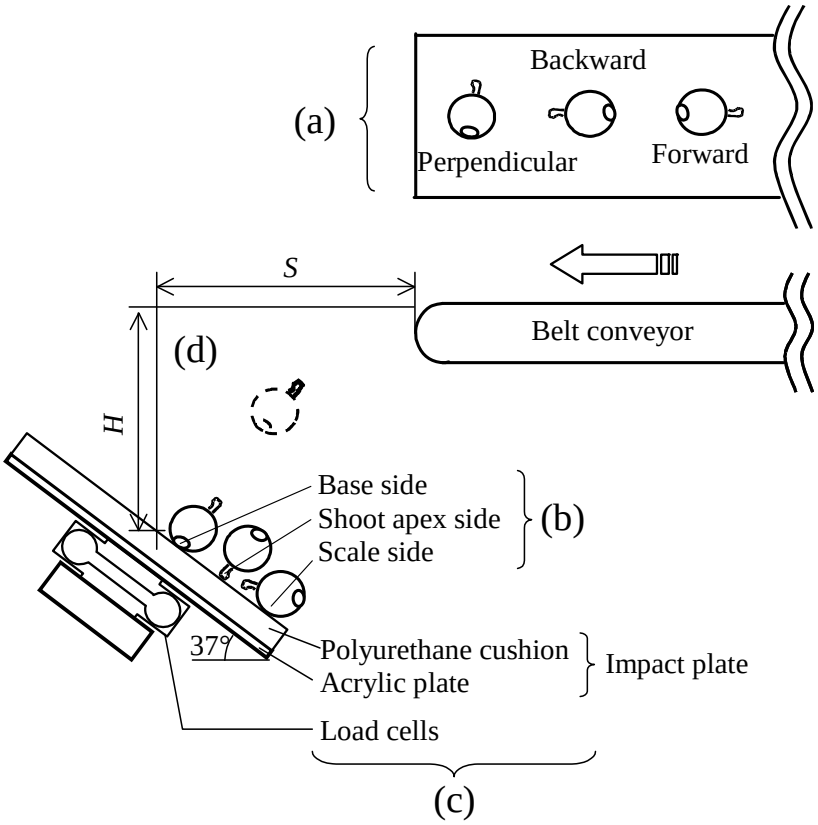

Fig.1 - (a) Three arrangements of onion bulbs on the conveyor, (b) patterns of incidence of the bulbs on the impact plate, (c) components of the yield sensor, (d) clearance, defined by the vertical and horizontal distances (*H*, *S*) from the output edge of the conveyor to the centre of the surface of the impact plate.

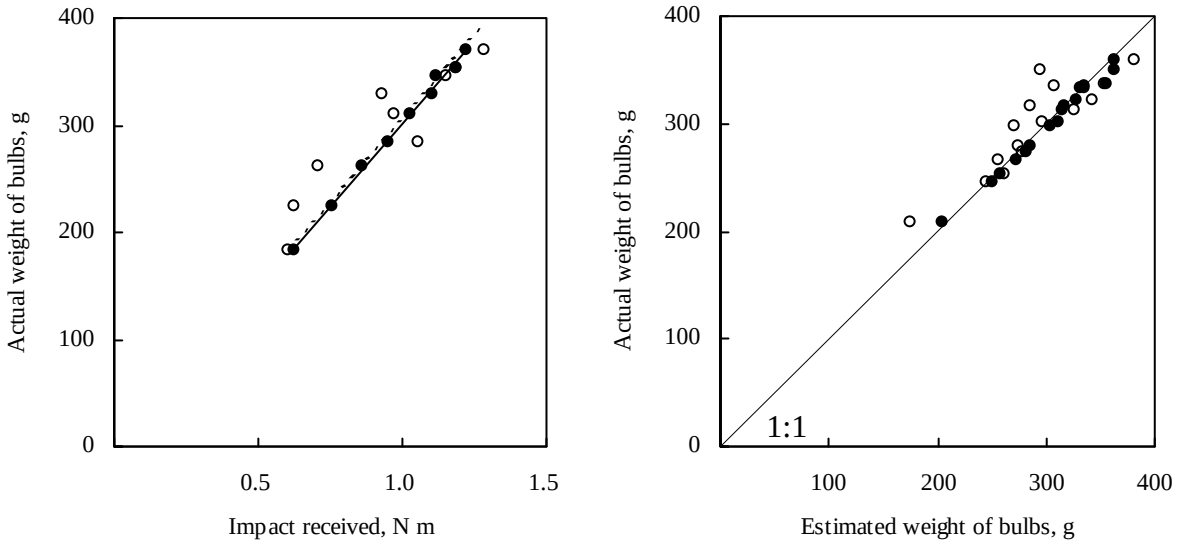

Fig. 2 - Examples of calibration (left panel) and validation (right panel) plots at the high clearance, forward direction of bulbs: ○ = 0 mm cushion, ● = 30 mm cushion; dotted and solid regression lines for 0 mm and 30 mm cushions, respectively (left panel).

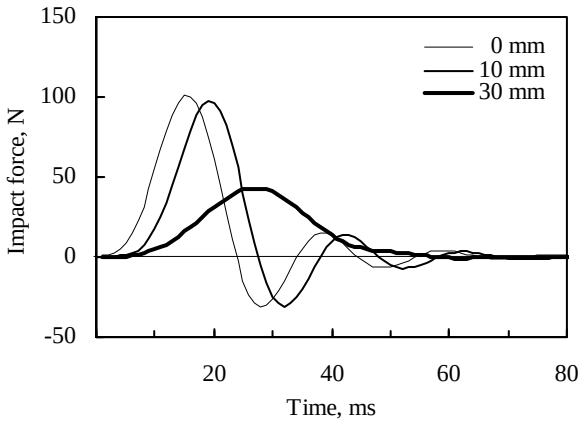

Fig. 3 - Transient response to impact of a 284 g bulb on cushions of different thicknesses, with cut-off frequency of low-pass filter at 50 Hz.